On the use of second-generation wavelets to combine a gravimetric quasigeoid model with GPS-levelling data

A. Soltanpour[1], H. Nahavandchi[1], W.E. Featherstone[2]

1. Department of Geomatics, Norwegian University of Science and Technology, N-7491, Trondheim, Norway; tel: +47 735 94580; fax +47 735 97021; email: ali.soltanpour@ntnu.no; hossein.nahavandchi@ntnu.no

2. Western Australian Centre for Geodesy, Curtin University of Technology, GPO Box U 1987, Perth WA 6845, Australia; email: w.featherstone@curtin.edu.au

Abstract. The merging of a gravimetric quasigeoid model with GPS-levelling data using second-generation wavelets is considered so as to provide better transformation of GPS ellipsoidal heights to normal heights. Since GPS-levelling data are irregular in the space domain and the classical wavelet transform relies on Fourier theory, which is unable to deal with irregular data sets without prior gridding, the classical wavelet transform is not directly applicable to this problem. Instead, second-generation wavelets and their associated lifting scheme, which do not require regularly spaced data, are used to combine gravimetric quasigeoid models and GPS-levelling data over Norway and Australia, and the results are cross-validated. Cross-validation means that GPS-level-ling points not used in the merging are used to assess the results, where one point is omitted from the merging and used to test the merged surface, which is repeated for all points in the dataset. The wavelet-based results are also compared to those from least squares collocation (LSC) merging. This comparison shows that the second-generation wavelet method can be used instead of LSC with similar results, but the assumption of stationarity for LSC is not required in the wavelet method. Specifically, it is not necessary to (somewhat arbitrarily) remove trends from the data before applying the wavelet method, as is the case for LSC. It is also shown that the wavelet method is better at decreasing the maximum and minimum differences between the merged geoid and the cross-validating GPS-levelling data.

Correspondence to: A. Soltanpour

Keywords: Quasigeoid. Geoid. GPS-levelling. Second-generation wavelets. Lifting scheme. Cross-validation. Least squares collocation (LSC)

1. Introduction

The relation among geoid (N), ellipsoidal (h) and orthometric heights (H) is

$$h - H - N = e \tag{1a}$$

Likewise, the relation among quasigeoid (ζ), ellipsoidal (h) and normal heights (H^*) is

$$h - H^* - \zeta = e' \tag{1b}$$

where h are usually obtained from GPS observations, and H and H^* are derived from geodetic levelling. Acknowledging plumbline curvature and neglecting all data errors, the values of e and e' should be zero, but rarely are zero due to various errors, such as long-wavelength geoid or quasigeoid errors, systematic errors in levelling networks, and geodynamic effects like post-glacial rebound (e.g., Ekman 1989). As such, there are always discrepancies between a gravimetric (quasi)geoid model and the heights from GPS-levelling.

Therefore, using a gravimetric quasigeoid/geoid model to transform GPS ellipsoidal heights to normal/orthometric heights does not always yield results that are compatible with the local vertical datum (e.g., Featherstone 1998; Nahavandchi and Soltanpour 2005). To improve this transformation, the gravimetric (quasi)geoid model can be fitted to the GPS-levelling data. The new combined surface (importantly which is no longer the classical (quasi)geoid) can then be used to give a more direct height transformation.

For many years, GPS-levelling was used almost exclusively for testing gravimetric (quasi)geoid models on land, but as geoid computation techniques improve, these reveal discrepancies (i.e., non-zero e and e'). As such, numerous studies have been dedicated to combining a gravimetric (quasi)geoid and GPS-levelling data. For example, Heiskanen and Moritz (1967), Sideris et al. (1992) and Sideris (1993) used a trigonometric four-parameter surface to minimize biases and very long-wavelength differences between geoid and GPS-levelling data.

More recently, a wide variety of higher-order parametric and non-parametric surfaces have been used for this purpose, such as artificial neural networks (Kavzoglu and Saka 2005), spline interpolation (e.g., Featherstone 2000), least squares collocation (LSC) (e.g., Iliffe et al. 2003, Featherstone and Sproule 2006), Kriging (e.g., Duquenne et al. 2004; Nahavandchi and Soltanpour 2004), combined least squares adjustments (e.g., Jiang and Duquenne 1996; Kotsakis and Sideris 1999; Marti et al. 2002; Fotopoulos 2005), and various other surfaces. Suffice it to say, there are numerous surface-fitting options, each with their own advantages and disadvantages, which will not be discussed nor debated here.

This paper adds to the above list of fitting options by describing the merging of gravimetric quasigeoid models with GPS-levelling using second-generation wavelets, supplemented with case studies in Norway and Australia.

- In Australia, there is an inconsistency between AUSGeoid98 (Featherstone et al. 2001) and the Australian Height Datum (AHD; Roelse et al. 1971). In addition to the above-mentioned factors, these inconsistencies are mostly due to a north–south trend, which is mostly caused by an un-modelled sea surface topography on the 30 tide gauges used in the AHD (Featherstone 2002, 2004).
- In Norway, although the recent gravimetric quasigeoid over Norway, OCTAS02 (Omang et al. 2004), exhibits a shift compared to the GPS-levelling data, it has a good relative precision compared to its Australian counterpart. In Norway, heights are referred to the NN1954 Norwegian height system, which is based on precise levelling, conducted during 1916–1954 and adjusted in 1956 (Lysaker 2003), but the height system remains ambiguous.

Acknowledging these inconsistencies has become necessary to fit gravimetric quasigeoid models to GPS-levelling as an interim solution to GPS-heighting until the AHD (1971) and NN1954 vertical datums and the respective quasigeoid models are refined.

In this regard, wavelets are a very powerful tool in numerical data analysis. They are widely used in image and signal processing for de-noising, filtering and compressing signals (e.g., Mallat 1999). The advantage of wavelets over Fourier transforms is their space-localization property in the frequency domain that lets them detect local as well as global frequencies. Wavelets have been used in several geodetic studies

(e.g., Freeden and Schneider 1998, 2005; Keller 2000; Zhou et al. 2001; Lio and Sideris 2003; Kuroishi and Keller 2005; Hu et al. 2005), which demonstrate some advantages over traditional spectral-analysis techniques.

However, classical wavelets are based on Fourier theory, which requires regularly spaced/sampled data, whereas GPS-levelling observations are not distributed in this way. Second-generation wavelets (Sweldens 1997) are thus a more attractive option for our purpose because they do not require regularly spaced data. In addition, they are conceptually superior to LSC, because they do not require the stationarity assumption, which is not always fulfilled in real datasets. In practice, LSC often requires the a priori removal of a trend to attempt to achieve stationarity, which can be subjective (e.g., planes or any higher-order surfaces could be used).

2 Wavelets and multiscale decomposition

In general, wavelet analysis is based on two basic functions: the scaling function $\varphi(x)$ and the wavelet, or detail, function $\psi(x)$. A classical wavelet system comprises an infinite collection of translated and scaled versions of $\varphi(x)$ and $\psi(x)$ according to (e.g., Antoniadis 1997)

$$\begin{aligned} \varphi_{j,k}(x) &= 2^{\frac{j}{2}}\varphi(2^j x - k) \qquad j,k \in Z \\ \psi_{j,k}(x) &= 2^{\frac{j}{2}}\psi(2^j x - k) \qquad j,k \in Z \end{aligned} \tag{2}$$

Considering the function $f(x)$ and the mother wavelet $\psi(x)$, $f(x)$ can be expressed as a linear combination of basis functions $\psi_{j,k}(x)$ as:

$$f(x) = \sum_{j,k} a_{j,k}\psi_{j,k}(x) \tag{3}$$

where $a_{j,k}$ are the detail or wavelet coefficients.

Unlike the Fourier transform, which is only localized in the (global) frequency domain, the wavelet transform is localized in both the space (or time) and frequency domains. This property introduces wavelet

analysis as a powerful tool to deal with signals whose spectral content changes in space (or time). In essence, a high frequency at x_0 will only affect the coefficient $\psi_{j,k}$ corresponding to the location and frequency at x_0. Readers interested in the mathematical details of classical wavelets are referred to Mallat (1999), Daubechies (1992) and Antoniadis (1999).

Considering a multi-resolution analysis (MRA) in L_2, a sequence of subspaces $\{V_j\}_{j\geq 0}$ is defined such that

$$V_j \subset V_{j+1} \text{ and clos} \bigcup_{j=0}^{\infty} V_j = L_2 \tag{4}$$

Besides, there are complement spaces W_j so that $V_{j+1} = V_j \oplus W_j$. Therefore, a fine-resolution space V_j can be decomposed into a coarser space and complement space,

$$V_j = V_0 \oplus \bigoplus_{i=0}^{j-1} W_i \tag{5}$$

This is called multiscale decomposition (MSD).

The spaces V_j and W_j are spanned by scale $\{\varphi_{j,k}\}$ and wavelet $\{\psi_{j,k}\}$ functions, respectively. The scale and wavelet functions at a coarser level are computed from scale functions at a finer level using some refinement coefficients h_{jlk} and g_{jlm} such that

$$\varphi_{j,k} = \sum_l h_{jlk}\, \varphi_{j+1,k} \quad \text{and} \quad \psi_{j,m} = \sum_l g_{jlm}\, \varphi_{j+1,l} \tag{6a}$$

or

$$\phi_j = \phi_{j+1} H_j \quad \text{and} \quad \Psi_j = \phi_{j+1} G_j \tag{6b}$$

where ϕ_j and Ψ_j are row vectors containing the functions $\varphi_{j,k}$ and $\psi_{j,m}$, respectively, and H_j and G_j are the refinement matrices.

In biorthogonal cases, different basis functions are used for the decomposition and reconstruction of a signal. The ϕ_j and Ψ_j are used in the reconstruction stage and their duals, $\tilde{\phi}_j$ and $\tilde{\Psi}_j$, are used for decomposition. Any function $f(x)$ can now be expressed by wavelet basis functions as

$$f(x) = \sum_k s_{j_0,k} \varphi_{j_0,k}(x) + \sum_{j,k} d_{j,k} \psi_{j,k}(x) \tag{7}$$

where

$$s_{j0,k} = \langle f, \tilde{\varphi}_{j_0,k} \rangle \quad \text{and} \quad d_{j,k} = \langle f, \tilde{\psi}_{j,k} \rangle \tag{8}$$

and the dual operators $\tilde{H}_j$ and $\tilde{G}_j$ are defined as

$$\tilde{\phi}_j = \tilde{\phi}_{j+1}\tilde{H}_j \quad \text{and} \quad \tilde{\Psi}_j = \tilde{\phi}_{j+1}\tilde{G}_j \tag{9}$$

In this case, the biorthogonality conditions on the refinement matrices and their duals (i.e., filters) would be

$$\tilde{H}_j^* H_j = I, \qquad \tilde{G}_j^* H_j = 0$$

$$\tilde{H}_j^* G_j = 0, \qquad \tilde{G}_j^* G_j = I \tag{10}$$

where * indicates the Hermitian conjugate and I is the identity matrix. Let $s_j = \{s_{j,k}\}$ and $d_j = \{d_{j,k}\}$. The forward wavelet transform is then given by

$$s_j = \tilde{H}_j^* s_{j+1} \qquad \text{and} \qquad d_j = \tilde{G}_j^* s_{j+1} \tag{11}$$

and the inverse transform is

$$s_{j+1} = H_j s_j + G_j d_j \tag{12}$$

Signals subjected to wavelet analysis are sometimes highly correlated. This is the case for GPS-levelling data, where for example systematic distortions occur in the levelling data tied to one vertical datum. Depending on the amount of correlation in the signal [here, the vales of e and e' in Eq. (1)], the wavelet coefficients will be small, and those below a certain threshold value can be set to zero. This allows the signal to be expressed by fewer coefficients, which is why wavelets are useful for image compression (e.g., the JPEG image format). The inverse wavelet transform can then be applied to the thresholded wavelet coefficients to recover the original signal without significant (depending on the threshold value) loss of information. In some cases, the resulting signal is de-noised when some frequencies have been filtered out during thresholding in the wavelet domain. Later in this paper, we shall investigate the role of thresholding in the merging of quasigeoid-GPS-levelling data.

3 Second-generation wavelets: a summary

As stated, the classical wavelet transform relies on the Fourier transform, so cannot be applied to irregularly spaced datasets. The simplest solution would be to grid the data and then apply the classical wavelet transform. However, during data gridding we lose some (mainly high-frequency) information and the geometric structure of the original observations; moreover, gridding is subject to aliasing. Sideris (1995) developed a technique to implement the Fourier transform on irregular datasets, but it still fundamentally relies on a regular grid where empty cells are set to zero or include interpolated data.

To deal with irregular datasets, second-generation wavelets have been developed by Sweldens (1997), which are not necessarily the translates and dilates of one function, as is the case for the classical wavelet. Second-generation wavelets are constructed based on a lifting scheme (Sweldens 1997), which works in the space domain and thus does not rely on Fourier transformation, and hence avoids gridding. As such, it preserves the geometry of the observations. The lifting scheme can be used where no Fourier transform is possible, such as for wavelets on bounded domains, wavelets on curves and surfaces, and wavelets on irregular data sets (Sweldens 1996). Therefore, second-generation wavelets are well suited to modelling the residuals in Eqs. (1) and (2).

Considering two initial pairs of biorthoginal filters as (H_j^o and G_j^o) and ($\tilde{H}_j^o$ and $\tilde{G}_j^o$), it is possible to improve their properties using the lifting scheme. The lifting scheme states that for any operator P_j, a new pair of biorthogonal filters can be found as (Delouille et al. 2003)

$$(H_j = H_j^o + G_j^o P_j, \quad G_j = G_j^o) \quad \text{and} \quad (\tilde{H}_j = \tilde{H}_j^o, \quad \tilde{G}_j = \tilde{G}_j^o - \tilde{H}_j^o P_j) \tag{13a}$$

which interchange the role of primal and dual filters, and for any operator U_j

$$(H_j = H_j^o, \quad G_j = G_j^o - H_j^o U_j) \quad \text{and} \quad (\tilde{H}_j = \tilde{H}_j^o + \tilde{G}_j^o U_j, \quad \tilde{G}_j = \tilde{G}_j^o) \tag{13b}$$

The operations in Eq. (13) are called the prediction and update steps, respectively.

Now we may consider the model

$$e_i = m(x_i, y_i) + n_i \tag{14}$$

where e_i from Eq. (1) is located at the two-dimensional location (x_i, y_i) and n_i is the noise in e_i . A wavelet-type transform, adapted to irregularly spaced two-dimensional data, is used to estimate the function $m(x_i, y_i)$. Some compactly supported scaling functions $\{\phi_J, \tilde{\phi}_J\}$ at the finest level (where *J* is the level of observation) are defined, and then the scaling and wavelet functions at coarser levels *j = J −1, J −2, ...* are obtained using Eqs. (6a) or (6b) and appropriate filters.

However, the output of second-generation wavelets may deliver unacceptable results. The problem is that the non-equispaced transform is unstable, i.e., far from orthogonal.

Consequently, small-magnitude coefficients may turn out to carry crucial information, while other large-magnitude coefficients may contain mostly noise (Jansen and Oonincx 2005). Indeed, since the basis is oblique (non-orthogonal), some large-scale features can leak into the small-scale part of the wavelet spectrum. This instability can be attenuated by a variance-normalization or update step. The minimum norm update operator is used here to keep the basis close to orthogonal by minimizing the update coefficients' norm (Delouille et al. 2003).

3.1. Lifting scheme in one dimension

It is instructive to first consider the one-dimensional case. The classical fast wavelet transform and second-generation wavelet transform are shown in Fig. 1. The classical wavelet transform starts by applying high-pass and low-pass filters on the original signal λ_j . The results are then downsampled to details or wavelet coefficients (γ_{j-1}) and a coarser version of original signal (λ_{j-1}). This process is repeated on λ_{j-1} to get γ_{j-2} and λ_{j-2}, then continues until it reaches γ_0 and λ_0 . This approach can be used in MRA, where a signal is spectrally analysed at different (space or time) scales.

The second-generation wavelet transform is based on the so-called lifting scheme and starts with the "lazy wavelet", which downsamples the signal to even and odd samples. The odd samples are then used to predict the even ones. The detail γ_{j-1} is the predicted value subtracted from the even sample. The details are then used to update the odd samples to keep the mean value of the signal unchanged.

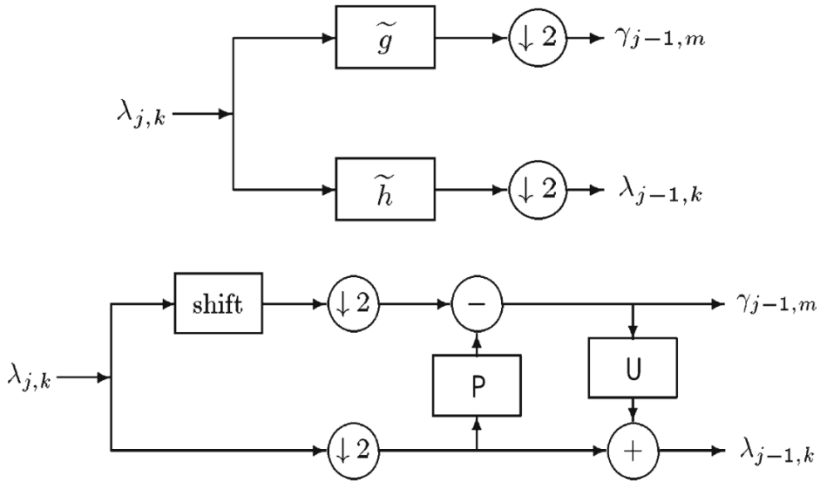

Fig. 1 Classical wavelet transform (*top*) and lifting scheme for the second-generation wavelet transform (*bottom*) (from Sweldens 1997)

Let $\lambda_{0,k} = f\ (k)$, $k \in Z$, be the original signal. The first approximation based on applying the lazy wavelet is

$$\lambda_{-1,k} = \lambda_{0,2k}\ ,\ k \in Z \tag{15}$$

and the details, or wavelet coefficients, are

$$\gamma_{-1,k} = \lambda_{0,2k+1} - \frac{1}{2}(\lambda_{-1,k} + \lambda_{-1,k+1}),\ k \in Z \tag{16}$$

If the signal is correlated, the wavelet coefficients ($\gamma_{i,j}$) are small and values below some threshold may be ignored (described later). In order to keep the mean of (λ) constant, the approximated values ($\lambda_{-1,k}$) must be updated using the detail or wavelet coefficients. Equation (15) is thus modified to

$$\lambda_{-1,k} += \frac{1}{4}(\gamma_{-1,k-1} + \gamma_{-1,k}),\ k \in Z \tag{17}$$

The above computations are represented schematically in Fig. 2. One can use a higher-order scheme to predict the odd indexed values from the even ones. For example, $\gamma_{j,2k+1}$ can be predicted based on cubic polynomial interpolation through the values $\gamma_{j,2k-1}$, $\gamma_{j,2k}$, $\gamma_{j,2k+1}$ and $\gamma_{j,2k+2}$. As such, there is some interpolation embedded in the second-generation wavelet technique, but this applies to the treatment of the wavelet coefficients only, and not the original data.

The inverse second-generation wavelet transform is simply applied by reversing the update and prediction steps.

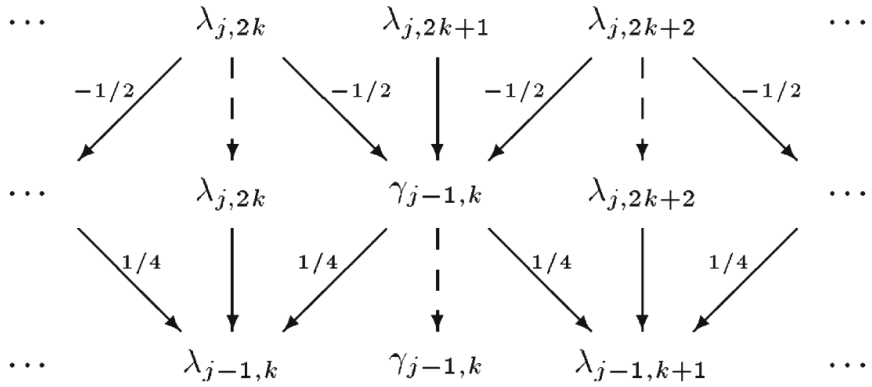

Fig. 2 Lifting scheme: computing coefficients $\gamma_{j-1,k}$ and then using them to lift $\lambda_{j-1,k}$ in one dimension (from Sweldens 1996)

3.2 Lifting scheme in two dimensions

In two dimensions, which applies to our case (cf. Eq. 14), the above one-dimensional splitting into odd and even samples is not possible. Therefore, a different spatial geometry should be used for constructing the second-generation wavelets and defining the neighborhoods. In our study, Delaunay triangulations and Voronoi tessellations are used for this purpose (cf. dos Santos and Escobar 2004). The benefit of using Delaunay and Voronoi methods [also known as triangulated irregular networks (TINs)] is that they preserve the spatial structure of the original GPS-levelling observations. This allows more detail to be used in areas of dense data, which would be smoothed out by gridding if classical wavelets were to be used.

Delaunay triangulation (Fig. 3) comprises triangles connecting the nearest-neighbour vertices (here, GPS-levelling points). The Delaunay triangulation is then used to build a Voronoi diagram: a set of cells, each of which contains the locations closer to a certain vertex than the others (Fig. 3). The edges of Voronoi polygons are bisectors of the sides of the Delaunay triangles (e.g., Delouille et al. 2003).

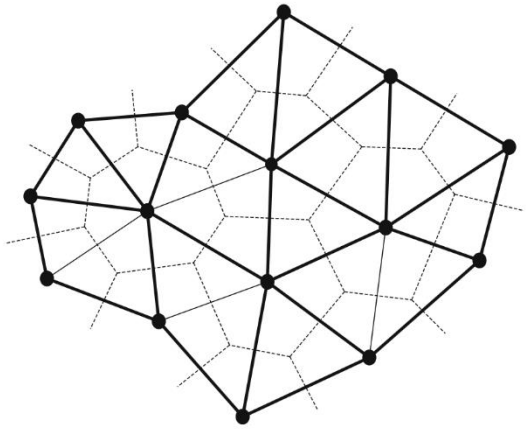

Fig. 3 Delaunay triangulation (*solid line*) and Voronoi tessellation (*dashed line*) in 2D space

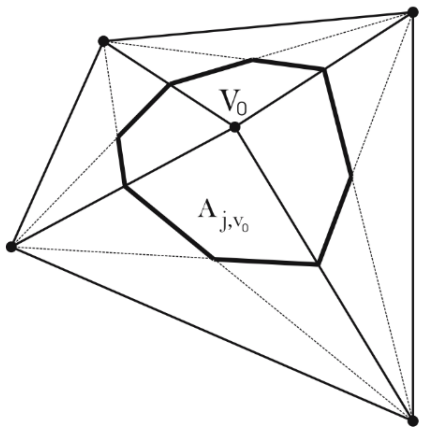

Fig. 4 Support of scaling function $\varphi_{j,v_0}(x)$ by a Voronoi cell associated with the vertex v_0

The wavelet scaling function $\varphi_{j_0,v_0}(x)$, corresponding to a vertex v_0 (Fig. 4), at the observation level is the characteristic function of the Voronoi cell of the vertex v_0 in which medians of the immediate neighboring triangles are used instead of the bisectors (Delouille et al. 2003).The area of support of the scaling function (A_{j,v_0}) for the vertex v_0 is thus equal to integral of scaling function $\varphi_{j,v_0}(x)$, and is shown in Fig. 4.

In two-dimensional cases, at any given scale j, only one scaling coefficient or observation corresponding to a certain vertex is predicted, and then that coefficient is used to update its neighbors (cf. the one-dimensional lifting scheme), as will be explained below. Choosing a vertex for prediction is based on the support of scaling functions at all vertices. The vertex v_0 that has the smallest support from the scaling function at each level is selected and predicted.

The initial filters of the two-dimensional lifting scheme are

$$G_j^o = \widetilde{G}_j^o = \{v_0\} \qquad \text{and} \qquad H_j^o = \widetilde{H}_j^o = \{N(v_0)\} \tag{18}$$

where $N(v_0)$ are neighboring points (vertices) of the vertex v_0. The detail/wavelet coefficient corresponding to the vertex v_0 is (Delouille et al. 2003):

$$d_{j,v_0} = \widetilde{G}_j^* s_{j+1} = \widetilde{G}_j^{o*} s_{j+1} - P_j \widetilde{H}_j^{o*} s_{j+1} = s_{j+1,v_0} - P_{j,N(v_0)} s_{j+1,N(v_0)} \tag{19}$$

where s_{j+1,v_0} and $s_{j+1,N(v_0)}$ are the observations at v_0 and its neighbouring points ($N(v_0)$), respectively, and $P_{j,N(v_0)}$ are the prediction weights.

In our case, the vertices are the GPS-levelling points and their values ($s_{j,v}$) at the finest level are the algebraic differences between the gravimetric quasigeoid model and GPS-levelling data [i.e., e' in Eq. (1b)]. The detail/wavelet coefficients are the differences between the wavelet scaling coefficients and their predicted values (Eq. 19). The number of neighboring points used in prediction can be varied, and depends on the method of prediction, which can be, e.g., a plane or a polynomial of degree *n*. As for the one-dimensional case, the interpolation applies to the wavelet coefficients, which preserves the geometry of the observations.

After predicting the scale coefficient at v_0 and subtracting it from the observed value (Eq. 19), it is replaced with the computed detail, and then that vertex is eliminated from the Delaunay triangulation. Another Delaunay triangulation is then applied on the remaining data and a new set of Voronoi polygons built. The area previously occupied by φ_{j+1,v_0} is now taken by a new area corresponding to its neighbours ($\varphi_{j,N(v_0)}$). In this study, planar and second-order surfaces, determined using unweighted least-squares, are used for the coefficient prediction. The immediate neighbours (first ring) are used for the linear prediction, and both the first- and second-ring neighbors are used for the second-order polynomial prediction (Fig. 5).

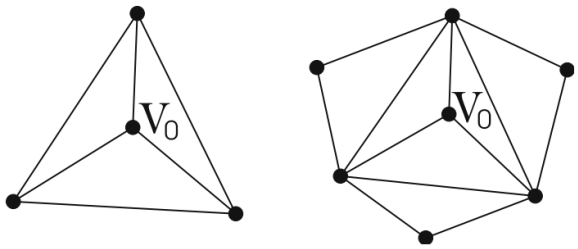

Fig. 5 Immediate/first-ring neighbours (left); first- and second-ring neighbours (right)

The prediction step is followed by an update step, which updates the scaling coefficients at neighboring vertices (Eq. 13b),

$$s_{j,N(v_0)} = \widetilde{H}_j^* s_{j+1} = \widetilde{H}_j^{0*} s_{j+1} + U_j \widetilde{G}_j^* s_{j+1} = s_{j+1,N(v_0)} + U_j d_{j,v_0} \tag{20}$$

The update coefficients U_j are computed to keep $\sum_k s_{j,k} A_{j,k}$ unchanged. This is equivalent to providing the primal wavelet ψ_{j,v_0} with one vanishing moment (e.g., Mallat 1999). To achieve this, we have to impose that (Jansen et al. 1999)

$$A_{j+1,\,v_0} = \sum_{k \in N(v_0)} A_{j,k}\, u_{j,k} \tag{21}$$

Update coefficients can then be computed using the minimum norm update operator (Jansen et al. 1999)

$$u_{j,k} = \frac{A_{j,k} A_{j+1,\,v_0}}{\sum_{l \in N(v_0)} A_{j,l}^2} \tag{22}$$

Since the update step modifies the primal wavelet basis functions, large update coefficients will cause the lifted wavelet function to be close to the space spanned by scaling function at a coarser level. This means that the wavelet and scaling function would be far from orthogonal, as stated earlier. The minimum norm update operator (Eq. 22) avoids this instability by minimizing the update coefficients (Delouille et al. 2003), thus making it more suited to our problem of merging quasigeoid and GPS-levelling data.

3.3 Thresholding

When applying thresholding to second-generation wavelets, any coefficients smaller than a specified threshold value are replaced by zeros (Sweldens 1996). This is analogous to multiple regression equations. Therefore, the signal of interest is expressed using the remaining coefficients. Finding an optimal threshold value is an important part in smoothing or filtering. A small threshold will cause the output to be the same as noisy input signal, and a large threshold introduces the risk of losing real signal in addition to noise.

The following model of data (corrupted by noise, *n*) and its wavelet transform are considered:

$$y = f + n \tag{23}$$

$$\omega = \widetilde{W} y \tag{24}$$

where $\widetilde{W}$ is the forward wavelet transform and ω is the vector of wavelet coefficients. The coefficients below a threshold value λ are replaced with zero and the others are left untouched (hard thresholding) or shrunk by the factor λ (soft thresholding). Applying the inverse wavelet transform to the thresholded coefficients yields the filtered data

$$y_\lambda = W\omega_\lambda \tag{25}$$

An optimal threshold value can be computed by minimizing the generalized cross-validation (GCV) function (Jansen and Bultheel 1999). Note that this is not the same as the cross-validation in Sect. 4.1.

$$\mathrm{GCV}(\lambda) = \frac{1/N\|\omega-\omega_\lambda\|^2}{(N_0/N)^2} \tag{26}$$

where N is the number of all coefficients (not to be confused with the geoid height), N_0 is the number of coefficients replaced with zero during thresholding step, and ω and $\widetilde{\omega}$ are vectors of the original and thresholded coefficients, respectively. GCV is a threshold that minimizes the MSE (mean square error) of the function with respect to the data (Jansen and Bultheel 1999).

Because the standard deviation of each coefficient is different for the coefficients computed by the second-generation wavelet transform (Jansen and Bultheel 1999), they must be normalized before thresholding, as follows. If the covariance of the data (C) is known, the variances of coefficients can be computed by

$$D = \widetilde{W}C\widetilde{W}^T \tag{27}$$

where the superscript T indicates matrix transposition. The normalized coefficients can then be computed by dividing them by their standard deviations

$$\widetilde{\omega}_i = \frac{\omega_i}{\sqrt{D_{ii}}} \tag{28}$$

To verify the efficiency of the GCV method for finding the optimal threshold, we also look for an optimal threshold value by considering the standard deviation of results after applying the cross-validation technique [Sect. 4.1, not Eq. (26)]. In this case, different threshold values are trialled, and the maximum threshold is selected that gives the minimum standard deviation in the cross-validation with GPS-levelling data. The detail/wavelet coefficients below this threshold are ignored because they are assumed to contain unnecessary high-frequency information or noise, subject to the problem of possible leakage due the non-orthogonality of the second-generation wavelet (discussed earlier). Some similarity can be seen between this method and LSC, where we look for the signal and neglect the noise to find a smoothed surface.

4 Numerical Experiments, Results and Analysis

4.1 Cross validation

The cross-validation technique is a well-known approach in areas such as soil science, and is described in Fotopoulos (2003) and Featherstone and Sproule (2006) for the case of fitting gravimetric quasigeoid models to GPS-levelling data. To summarize, one GPS-levelling point is omitted from the merged solution, then the difference between the resulting merged quasigeoid-type surface and the GPS-levelling height at that unused point is computed. This is repeated for all GPS-levelling points in the dataset to give a sample from which descriptive statistics are computed.

The benefit of this approach is that the same data are not used twice; i.e., once to compute the merged surface, then again to test it. As such, we believe that it gives a more realistic and arguably more independent indication of the performance of the merged surface. In the case of our second-generation wavelet merging, the Delaunay triangulation and Voronoi cells are changed every time a point is omitted and used for cross-checking. This is repeated for all points in the dataset. While this is time consuming for both methods, it only needs to be done during the tests, then all data used with the optimal parameters to produce the final merged quasigeoid-type 'product'.

4.2 Data description

The two case-study regions of Norway and Australia were chosen principally for reasons of convenience to the authors, but they also exhibit different spatial densities of GPS-levelling data [1,724 stations in Norway (Fig. 6) and 254 stations in Australia (Fig. 7)]. Considering the areas of two countries (Australia is ~ 24 times bigger than Norway), the GPS-levelling data in Norway are much more dense, especially in the south. It will be shown later that, as expected for the second-generation wavelet technique, the denser the GPS-levelling data, the better the results.

The most recent publicly available Australian quasigeoid model, AUSGeoid98 (Featherstone et al. 2001), which is on a 2 by 2 arcmin grid, and the latest Norwegian quasigeoid model, OCTAS02 (Omang et al. 2004), which is on a 6 by 3 arcmin grid, were used in this study. The gravimetric quasigeoid heights were

bilinearly interpolated to the GPS-levelling points. The levelled heights refer to the AHD (Roelse et al. 1971) and NN1954 (Lysaker 2003) local vertical datums.

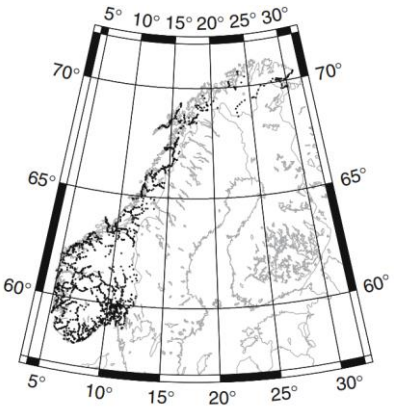

Fig. 6 Spatial distribution of GPS-levelling stations in Norway (Lambert projection)

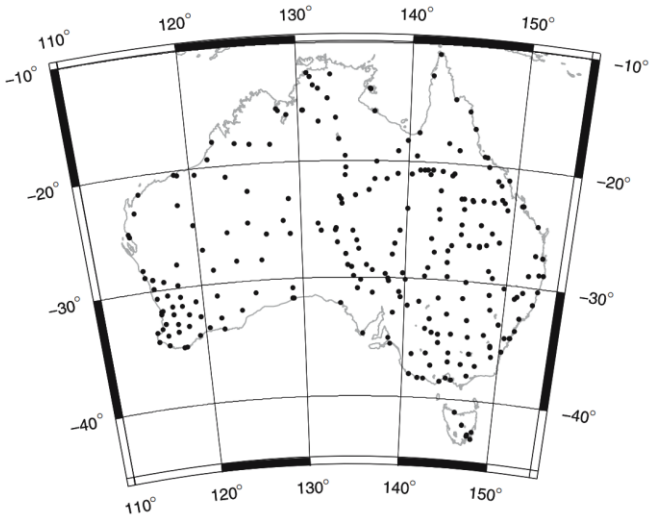

Fig. 7 Spatial distribution of GPS-levelling stations in Australia (Lambert projection)

The AHD uses a variant of the normal-orthometric height system, which is based on a truncated formula (Featherstone and Kuhn 2006). The height system used in NN1954 is rather ambiguous (Lysaker 2003), but will be assumed to be a normal height system. As such, the heights on each local vertical datum will have to be assumed compatible with each respective quasigeoid model, notwithstanding the various errors affecting their practical realization (see the Sect. 1). Finally, the GPS-derived ellipsoidal heights in Norway are referred to the EUREF89 datum and those in Australia refer to the ITRF2000 datum.

In this study, the variance of all these observations will be assumed zero, which is unrealistic but we do not have any reliable variance information at present. Also, since we seek a merged surface that makes $h - H^* - \zeta = e' = 0$ [cf. Eq. (1b)], which is enforced by assuming zero variance.

4.3 LSC merging

For the sake of comparison, and to show the efficiency of the second-generation wavelet method, LSC was also applied to the same datasets. Since covariance functions are generally not available, they have to be determined empirically (e.g., Moritz 1980), and then an analytic function fit to them in order to apply LSC. Normally, only isotropic (i.e., azimuth independent) covariance functions are considered, which is not the case with second-generation wavelets. Figure 8 shows empirical covariances computed from the Norwegian and Australian quasigeoid-GPS-levelling differences [e in Eq. (1b)], as well as an exponential analytical covariance function fitted to them using unweighted least squares. From Fig. 8, the empirical covariances decay faster in Norway (correlation length of 200 km) than in Australia (correlation length of 1,000 km), which reflects the spatially more dense data in Norway. Note that the correlation length for Australia differs from the 2,500 km calculated in a different way by Featherstone and Sproule (2006). The correlation lengths of 200 and 1,000 km were used for Norway and Australia, respectively.

The difference between empirical and analytic covariance functions at zero-distance was taken to be the variance of the noise, which gave ±3.6 cm for Norway and ±11.4 cm for Australia. The smaller noise for Norway indicates both a better dataset and a better initial fit of OCTAS02 to the EUREF89-NN1954 data (i.e., gravimetric quasigeoid to the GPS-levelling) than the AUSGeoid98-ITRF2000-AHD (1971) data. Note that a planar surface had to first be removed from the data before the covariance functions were determined, unlike the second-generation wavelet method.

The LSC results were evaluated using the cross-validation approach (Sect. 4.1), and the results will be presented in Sect. 4.4, together with those obtained from the second-generation wavelet approach.

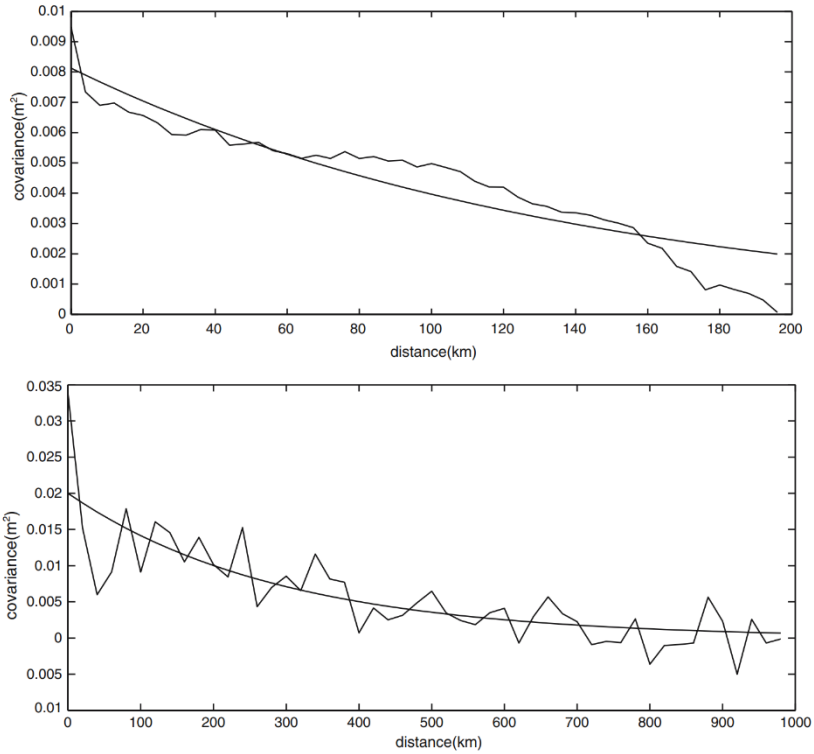

Fig. 8 Empirical covariances and fitted exponential analytical covariance function (*top*: Norway, *bottom*: Australia)

4.4 Wavelet merging

The second-generation wavelet transform based on the lifting scheme (Sect. 3.2) was applied to the Norwegian and Australian quasigeoid-GPS-levelling differences. Both planar and second-degree polynomial surfaces were tested for detail prediction, and the resulting wavelet coefficients were first normalized using Eq. (28). Because the covariance of the observations is unknown, $C = \sigma^2 I$ is assumed as their covariance matrix, where σ is the standard deviation of the noise.

These normalized coefficients were soft-thresholded with the optimal threshold value computed from the GCV method (Eq. 26), which gave (dimensionless) values of 0.0040 for Norway and 0.0084 for Australia. As for the LSC covariance function, the larger value for Australia indicates a combination of poorer data and a poorer initial fit of the AUSGeoid98- ITRF2000-AHD data. To verify the threshold values computed using GCV (Eq. 26), a range of different threshold values were also applied, and assessed using the GPS-levelling cross-validation technique (Fig. 9). In Norway, the standard deviation of the cross-validation increases with increasing threshold. In Australia, it decreases until threshold of 0.16 and increases after that. The first ten

threshold values, their corresponding cross-validation standard deviation, and the number of thresholded (removed) wavelet coefficients for Norway and Australia are summarized in Table 1. Comparing the values in Table 1 with the values obtained from GCV method (0.0040 for Norway and 0.0084 for Australia) shows that the GCV method was successful in finding the optimal threshold value for Norway, but not in Australia. Assuming 0.5 mm as an acceptable tolerance for the standard deviation, the maximum threshold value of 0.25 was selected as the optimal value for both Norway and Australia (marked in bold in Table 1). The normalized coefficients were then soft-thresholded using this value, and then the inverse wavelet transformation was applied to give the (slightly smoothed) merged surface.

The final surfaces (for a threshold of 0.25) were then validated with the unused GPS-levelling points based on the cross-validation method (Sect. 4.1). The results in both absolute and relative senses (cf. Featherstone 2001) are summarized in Tables 2, 3, 4 and 5. All possible baselines between GPS-levelling points were considered in relative validation (i.e., 32,131 and 1,485,226 baselines for Australia and Norway, respectively). Table 4 includes the cross-validation statistics for the LSC combination by Featherstone and Sproule (2006), which used 253 of the same GPS-levelling points (one value was rejected as an outlier). In terms of standard deviation of the cross-validated differences after fitting, the soft-thresholded second-generation wavelet method is slightly better than LSC in Australia and slightly worse in Norway. Considering the maximum and minimum columns in Tables 2 and 4, however, wavelets have been more successful than LSC at decreasing the maximum and minimum differences (ignore the last row of Table 4, which rejected one suspected outlier). Both sets of results in Tables 4 and 5 show proportionally more improvement in Norway ($\sim$ 75%) than in Australia ($\sim$ 50%), which is due mostly to the spatially denser GPS-levelling data in Norway. In Tables 2, 3, 4 and 5, the linear and second-order detail prediction in the second-generation wavelets yielded very similar results, with the second-order method being slightly worse in Norway.

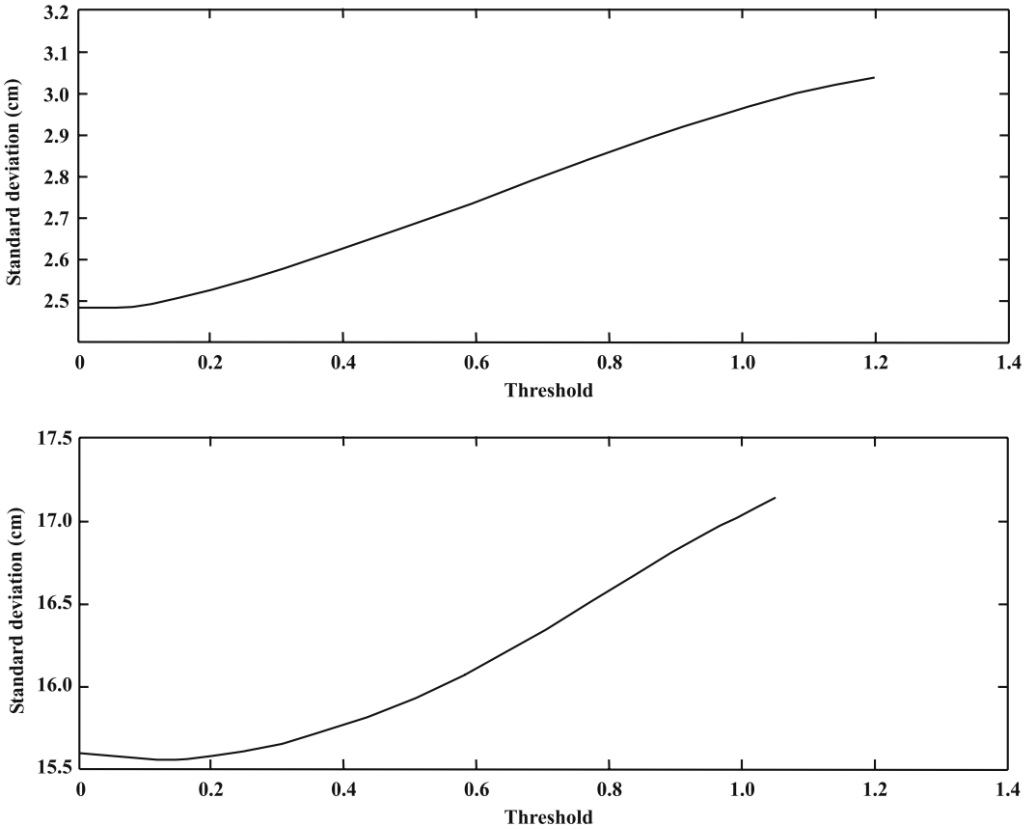

Fig. 9 Standard deviation of the cross-validation versus threshold values for Norway (*top*) and Australia (*bottom*); (linear wavelet coefficient prediction)

Table 1 The first ten threshold values, their corresponding cross-validation standard deviation (SD), and the number of thresholded coefficients for Norway and Australia (linear and second-order wavelet coefficient prediction)

Threshold	0.00	0.05	0.10	0.15	0.20	**0.25**	0.30	0.35	0.40	0.45
SD for Norway with linear prediction (cm)	2.48	2.48	2.49	2.50	2.52	**2.53**	2.57	2.59	2.62	2.65
Number of thresholded coefficients	0	140	252	369	497	**593**	687	750	822	889
SD for Norway with second-order prediction (cm)	2.48	2.49	2.49	2.51	2.52	**2.53**	2.56	2.60	2.63	2.67
Number of thresholded coefficients	0	141	254	373	499	**594**	686	748	818	882
SD for Australia with linear prediction (cm)	15.60	15.58	15.57	15.57	15.58	**15.61**	15.65	15.71	15.77	15.85
Number of thresholded coefficients	0	9	16	25	37	**46**	54	64	73	83
SD for Australia with second-order prediction (cm)	15.60	15.58	15.58	15.59	15.61	**15.63**	15.69	15.74	15.80	15.86
Number of thresholded coefficients	0	10	20	36	42	**49**	55	62	70	77

Table 2 Absolute cross-validation statistics for the merged quasigeoid-type surface at 1,724 GPS-levelling stations in Norway (cm)

	Mean	Max	Min	SD
OCTAS-02	−59.6	−30.8	−93.9	10.7
Wavelet (linear)	0.0	11.8	−11.8	2.5
Wavelet (second-order)	0.0	13.2	−11.9	2.5
LSC	0.0	13.3	−13.8	2.2

Table 3 Relative cross-validation statistics for the merged quasigeoid-type surface over 1,485,226 GPS-levelling baselines in Norway (cm)

	Mean	Max	Min	SD
OCTAS-02	−4.5	63.0	−60.5	14.6
Wavelet (linear)	0.0	23.8	−23.4	3.5
Wavelet (second-order)	0.0	22.8	−24.2	3.6
LSC	0.0	27.0	−23.9	3.1

Table 4 Absolute cross-validation statistics for the the merged quasi-geoid-type surface at 254 GPS-levelling stations in Australia (cm)

	Mean	Max	Min	SD
AUSGeoid98	7.6	86.5	−72.1	28.6
Wavelet (linear)	−0.1	50.1	−64.1	15.6
Wavelet (second-order)	0.1	50.0	−63.5	15.6
LSC	0.0	61.0	−56.7	15.5
Featherstone and Sproule (2006)	0.0	52.5	−60.3	15.6

Table 5 Relative cross-validation statistics for the merged quasigeoid-type surface over 32,131 GPS-levelling baselines in Australia (in cm)

	Mean	Max	Min	SD
AUSGeoid98	1.2	140.9	−158.7	40.4
Wavelet (linear)	2.4	112.2	−105.4	22.1
Wavelet (second-order)	2.6	111.4	−102.6	22.1
LSC	−1.6	103.8	−118.1	21.9

4. Summary, discussion and conclusion

To improve the accuracy of normal height determination on a local vertical datum by GPS, second-generation wavelets based on the lifting scheme, together with coefficient thresholding, has been introduced and implemented on the differences between gravimetric quasigeoid models and discrete GPS-levelling data over Norway and Australia. Unlike the classical wavelet transform, the second-generation wavelet can be applied directly to irregular datasets. The second-generation wavelet coefficients were soft-thresholded by a verified optimal threshold value from the GCV method, and then the inverse wavelet transformation was applied to give the merged surface. Importantly, this method is applicable to non-stationary data. As such, removing an a priori trend, which is necessary for LSC-based merging, is not required for the second-generation wavelet method.

The resulting merged quasigeoid-type surfaces were then cross-validated using GPS-levelling data not used to compute them. The results show that differences between the new surfaces and the unused GPS-levelling have decreased in both absolute and relative senses ($\sim$ 75% for Norway, and $\sim$ 50% for Australia). The differences in standard deviation between the results from LSC and wavelets are a few millimetres, but the wavelets have been more successful at decreasing the maximum and/or minimum differences than LSC. Therefore, second-generation wavelets are another alternative method that can be used for merging gravimetric quasigeoid/geoid models and GPS-levelling data on a local vertical datum.

Acknowledgements We greatly appreciate the reviewers, W. Freeden, W. Keller and C. Mayer, for patiently reading the paper and for their valuable comments. We would also like to thank D. Solheim (Norwegian National Mapping Authority) and O. Omang (Norwegian University of Life and Science) for providing GPS-levelling and quasigeoid data of Norway, respectively, and G. Johnston (Geoscience Australia) for providing the GPS-levelling data of Australia. The majority of work and all numerical computations were done while the first-named author was on a visiting fellowship at the Western Australian Centre for Geodesy, Curtin University of Technology. This work is a part of a project funded by the Norwegian Research Council grant 147618/V30, under the independent research program at the Division of Science and Technology, as well as Australian Research Council grant DP0211827.

References

Antoniadis A (1997) Wavelets in statistics: a review. Journal of the Italian Statistical Society 2: 97-138

Antoniadis A (1999) Wavelets in statistics: a review (with discussion). J Italian Stat Soc 6:97–144

Daubechies I (1992) Ten lectures on wavelets. SIAM, Philadelphia

Delouille V, Jansen M, von Sachs R (2003) Second generation wavelet methods for denoising of irregularly spaced data in two dimensions, Rep DP0305, Institut de Statistique, Universite Catholique de Louvain, Belgium

Duquenne H, Everaerts M, Lambot P (2005) Merging a gravimetric model of the geoid with GPS/levelling data: an example in Belgium. In: Jekeli C, Bastos L, Fernandes J (eds) Gravity, geoid and space missions. Springer, Berlin Heidelberg New York, pp 131–136

Ekman M (1989) Impacts of geodynamic phenomena on systems for height and gravity. Bull Géod 63:281–296

Featherstone WE (1998) Do we need a gravimetric geoid or a model of the base of the Australian Height Datum to transform GPS heights? Aust Surv 43(4):273–280

Featherstone WE (2000) Refinement of a gravimetric geoid using GPS and levelling data. J Surv Engg 126(2):27–56

Featherstone WE (2001) Absolute and relative testing of gravimetric geoid models using Global positioning system and orthometric height data. Comput Geosci 27(7):807–814. DOI: 10.1016/S0098- 3004(00)00169-2

Featherstone WE (2002) Prospects for the Australian Height Datum and geoid model. In: Ádám J, Schwarz K-P (eds) Vistas for geodesy in the new millennium. Springer, Berlin Heidelberg New York, pp 96–101

Featherstone WE (2004) Evidence of a north–south trend between AUSGeoid98 and AHD in southwest Australia. Surv Rev 37(291):334– 343

Featherstone WA, Kuhn M (2006) Height systems and vertical datums: a review in the Australian context. J Spatial Sci (in press)

Featherstone WE, Sproule DM (2006) Fitting AUSGeoid98 to the Australian height datum using GPS data and least square collocation: application of a cross validation technique. Surv Rev (in press)

Featherstone WE, Kirby JF, Kearsley AHW, Gilliland JR, Johnston GM, Steed J, Forsberg R, Sideris MG (2001) The AUSGeoid98 geoid model of Australia: data treatment, computations and comparisons with GPS-levelling data. J Geod 74:239–248. DOI: 10.1007/s001900100177

Fotopoulos G (2003) An analysis on the optimal combination of geoid, orthometric and ellipsoidal height data. PhD Thesis, University of Calgary, Alberta

Fotopoulos G (2005) Calibration of geoid error models via a combined adjustment of ellipsoidal, orthometric and gravimetric geoid height data. J Geod 79(1–3):111–123. DOI: 10.1007/s00190-005-0449-y

Freeden W, Schneider F (1998) An integrated wavelet concept of physical geodesy. J Geod 72(5):259–281. DOI: 10.1007/s001900050166

Freeden W, Schreiner M (2005) Spaceborne gravitational field determination by means of locally supported wavelets. J Geod 79(8):431– 446. DOI 10.1007/s00190-005-0482-x

Heiskanen W, Moritz H (1967) Physical geodesy. Freeman, San Francisco

Hu XG, Liu LT, Hinderer J, Sun HP (2005) Wavelet filter analysis of local atmospheric pressure effects on gravity variations. J Geod 79(8):447–459. DOI: 10.1007/s00190-005-0486-6

Iliffe JC, Ziebart M, Cross PA, Forsberg R, Strykowski G, Tscherning CC (2003) OGSM02: a new model for converting GPS-derived heights to local height datums in great Britain and Ireland. Surv Rev 37(290):276–293

Jansen M, Bultheel A (1999) Smoothing irregularly spaced signals using wavelets and cross validation. Report TW289, Department of Computerwetenschappen, Katholieke Universiteit Leuven, Belgium

Jansen M, Oonincx P (2005) Second generation wavelets and applications. Springer, Berlin Heidelberg New York

Jiang Z, Duquenne H (1996) On the combined adjustment of a gravimetrically determined geoid and GPS levelling stations. J Geod 70(8):505–514. DOI: 10.1007/s001900050039

Kavzoglu T, Saka MH (2005) Modelling local GPS/levelling geoid undulations using artificial neural networks. J Geod 78(9):520–527. DOI: 10.1007/s00190-004-0420-3

Keller W (2000) A wavelet solution to non-stationary collocation, In: Schwarz K-P (ed) Geodesy beyond 2000. Springer, Berlin Heidelberg New York, pp 208–214

Kotsakis J, Sideris MG (1999) On the adjustment of combined GPS/levelling/geoid networks. J Geod 73:412–421. DOI: 10.1007/s001900050261

Kuroishi Y, Keller W (2005) Wavelet approach to improvement of gravity field – geoid modeling for Japan. J Geophys Res 110:B03402. DOI: 10.1029/2004JB003371

Lio Q, Sideris MG (2003) Wavelet evaluation of the Stokes and Vening Meinesz integrals. J Geod 77(5–6):345–356. DOI: 10.1007/s00190- 003-0333-6

Lysaker D (2003) An evaluation of the Norwegian height system NN1954, different gravity corrections and assumptions of the adjustment. MSc thesis, Norwegian University of Life and Science, Oslo

Mallat SG (1999) A wavelet tour on signal processing. Academic, New York

Marti U, Schlatter E, Brockmann E, Weget A (2002) The way to a consistent national height system for Switzerland. In: Adam J, Schwarz K-P (eds) Vistas for geodesy in the new millennium. Springer, Berlin Heidelberg New York, pp 90–95

Moritz H (1980) Advanced physical geodesy. Wichmann, Karlsruhe

Nahavandchi H, Soltanpour A (2004) An attempt to define a new height datum in Norway. The geodesy and hydrography days 2004, 4–5 November, Sandnes, Norway

Nahavandchi H, Soltanpour A (2005) Improved determination of heights using a conversion surface by combining gravimetric quasi/geoid and GPS-levelling height differences. Studia Geophysica et Geodaetica (in press)

Omang OCD, Solheim D, Forsberg R (2004) New geoid models in the northern North Atlantic based on adjusted gravity data and new geopotential models. Geophys Res Abstracts 6:05962, SRef-ID: 1607- 7962/gra/EGU04-A-05962

Roelse A, Granger HW, Graham JW (1971) The adjustment of the Australian levelling survey 1970–1971 Technical Report 12, Division of National Mapping, Canberra, 81 pp

dos Santos NP, Escobar IP (2004) Discrete evaluation of Stokes's integral by means of Voronoi and Delaunay structures. J Geod 78(6):354– 367. DOI: 10.1007/s00190-004-0402-5

Sideris MG (1993) Tests of a gravimetric geoid in GPS networks. Surv Land Inf Syst 53(2):94–102

Sideris MG (1995) Fourier geoid determination with irregular data. J Geod 70(1):2–12

Sideris, MG, Mainville A, Forsberg R (1992) Geoid testing using GPS and levelling (or GPS testing using levelling and the geoid?). Aust J Geod Photogramm Surv 57:62–67

Sweldens W (1996) Wavelets and the lifting scheme: a 5 minute tour. Zeitschrift für Angewandte Mathematik und Mechanik 76(2): 41–44

Sweldens W (1997) The lifting scheme: a construction of second generation wavelets. SIAM J Math Anal 29(2):511–546. DOI: 10.1137/S0036141095289051

Zhou YH, Zheng DW, Liao XH (2001) Wavelet analysis of interannual LOD, AAM, and ENSO: 1997–98 El Nino and 1998–99 La Nina signals. J Geod 75(2–3):164–168. DOI: 10.1007/s001900100173